JOURNAL OF CATALYSIS **143**, 275–285 (1993)

# Studies on Crystalline Microporous Vanadium Silicates

## IV. Synthesis, Characterization, and Catalytic Properties of V–NCL-1, a Large-Pore Molecular Sieve

K. RAMESH REDDY, A. V. RAMASWAMY, AND P. RATNASAMY

*National Chemical Laboratory, Pune-411008, India*

Received January 14, 1993; revised April 20, 1993

The synthesis and catalytic properties of V–NCL-1, a novel vanadium silicate, large-pore molecular sieve in various oxidation reactions, are described. The reactions include the oxidation of *n*-octane, cyclohexane, toluene, trimethylbenzenes, and naphthalene. In the as-synthesized form, most of the vanadium in V–NCL-1 is present as atomically dispersed and isolated $V^{4+}$ located in framework positions, though not necessarily in tetrahedral coordination. On calcination in air, the vanadium ions are oxidized to the pentavalent state. In addition, part of the vanadium leaves lattice locations and forms nonframework clusters. When the oxidized sample is reduced, $V^{4+}$ ions are formed again. The three-dimensional silicate structure of the molecular sieve is intact during all these treatments. Due to the presence of large pores, V–NCL-1 is able to oxidize bulky molecules such as mesitylene and naphthalene. Unlike their titanium analogs, vanadium silicates are able to oxyfunctionalize the primary carbon atoms in alkanes and the side chains in alkylaromatics.


## INTRODUCTION

Crystalline microporous vanadium silicates are a new class of materials wherein the oxidative property of vanadium could be combined with the shape-selective characteristics imparted by the micropore structure in which the vanadium is located. So far, only three vanadium-containing molecular sieves are known and well-characterized (*1–6*). Two of them are metallosilicates and belong to the medium-pore pentasil family viz., V–MFI (*1–4*) and V–MEL (*5*), respectively. The third, VAPO-5 is a metallophosphate molecular sieve (*6*). Our earlier communications on the vanadium silicate molecular sieves describe the synthesis, characterization, and catalytic activity of V–MEL samples with different Si/V ratios (*5, 7–10*). The possible location of vanadium atoms in the silicalite matrix and their catalytic properties in the oxidation of different organic substrates have been demonstrated. In contrast to titanium silicalites, they are able to oxyfunctionalize the primary carbon atom in *n*-alkanes and side chains of alkyl aromatics (*8*), are more active in the oxidation of alcohols to carbonyl compounds, and are greatly influenced by the nature of solvents used in the reactions (*8, 10*). These studies have so far been restricted to medium-pore structures.

Recently, we have synthesized and characterized a new large-pore zeolite, designated as NCL-1 with a Si/Al ratio of 20 and above, and its Al-free silica polymorph (*11*). The adsorption and catalytic properties of NCL-1 are characteristic of zeolites with pore-openings constituted by 12-membered tetrahedra. The effective pore-diameter of NCL-1 (from adsorption and diffusivity measurements) is close to that of mordenite (~0.7 nm) (*11*). The possibility of incorporating vanadium into Si–NCL-1 structure has led to the synthesis, for the first time, of a vanadium-containing, large-pore molecular sieve, which has interesting applications in the oxidation of bulky hydrocarbons



0021-9517/93 $5.00

(*12*). In this communication, we describe our detailed studies on the synthesis of V–NCL-1, a novel, vanadium-containing large pore molecular sieve, its characterization, and its performance in the oxidation of *n*-octane, cyclohexane, toluene, xylenes, trimethylbenzenes, and naphthalene in the presence of aqueous $H_2O_2$.

## EXPERIMENTAL

### *Synthesis*

The silica polymorph of NCL-1 (sample A) and three vanadium silicate samples (B, C, and D) with Si/V molar (gel) ratios of 175, 96, and 48, respectively, were synthesized hydrothermally. The gel compositions (molar), used in the syntheses were as follows: $SiO_2/VO_2$ = 48 to $\infty$; $SiO_2/OH^-$ = 8.33; $SiO_2/RBr_2$ = 20, where $RBr_2$ is the organic template, hexamethylene bis(triethylammonium bromide) and $SiO_2/H_2O$ = 0.019.

Raw materials used in the synthesis were fumed silica (99.9%, Sigma, USA, S-5005), NaOH (AR grade), and $VOSO_4 \cdot 5H_2O$ (Loba Chemie., 98%). In a typical synthesis, 4.5 g of fumed silica was dissolved in NaOH solution (0.48 g of NaOH in 35 g of $H_2O$) under stirring for 1 h, after which an aqueous solution of $VOSO_4 \cdot 5H_2O$ (0.4 g of $VOSO_4 \cdot 5H_2O$ in 10 g $H_2O$) was added. This mixture was stirred for 1 h and then 1.71 g of organic template was added. After addition of the remaining water, the homogeneous reaction mixture was stirred for 2 h, and charged into a stainless steel autoclave. The crystallization was carried out under agitation at 443 K. The crystallization time for samples A to D (Si/V = $\infty$, 175, 96, and 48) were 4, 9, 12, and 16 days, respectively. After the crystallization, the product was filtered, washed with deionized water, dried at 383 K and calcined in air at 723 K. From thermogravimetric analysis, the amount of template that decomposed in air between 500 and 773 K is calculated to be 7.5, 6.9, 6.8, and 6.8 wt% for samples A, B, C, and D, respectively. The Si/Na ratio of the calcined samples are 33, 27, 24, and 20 for samples A, B, C, and D (see Table 2). And after washing the sample D with ammonium acetate the Si/Na ratio is 113. Most of the vanadium ions in non-framework positions were removed in the following manner: 1 g of the calcined vanadium silicate (sample D) was treated with 50 ml of 1 *M* ammonium acetate for 24 h at 300 K, washed with distilled water, dried and calcined in air at 723 K to give sample E.

The X-ray powder diffraction profiles of calcined and hydrated samples were recorded in a Rigaku (Model D-Max III VC) instrument using Ni-filtered Cu$K\alpha$ radiation and a graphite monochromator, in a step scan mode of 0.05° with 50 s accumulation time. The unit cell parameters were calculated after refinement of the XRD data using PDP 11 software (University of Trieste, Italy).

The chemical analyses of all the samples were performed either by wet chemical method using atomic absorption spectrometer (Hitachi, Japan) (Na and V) or using X-ray fluorescence spectrometer (Rigaku, model 3070) for solids after forming glassy beads in an induction furnace and standardization with reference materials. $N_2$ adsorption experiments of calcined and ammonium acetate-treated samples were carried out volumetrically in Omnisorb 100 CX (Coulter Corporation, USA) analyzer at liquid $N_2$ temperature. From the nitrogen adsorption data, apparent surface areas (BET), and mesopore areas (*t*-area) were calculated. *o*-Xylene and mesitylene sorption measurements were carried out gravimetrically in a Cahn electrobalance (Model 2000 G) at $p/p_0$ = 0.5 and at 298 K. The equilibrium adsorption levels were reached within 10 min, but the final sorption capacities were taken after 2 h. Framework IR spectra of calcined samples (in Nujol) were recorded in the region of 450–1300 $cm^{-1}$ with a Perkin–Elmer (Model 224) FTIR spectrometer. The ESR spectra of as-synthesized, calcined or reduced samples were recorded at 298 K in the X-band in a Bruker (Model ER 200 D) spectrometer using DPPH as calibrating material.

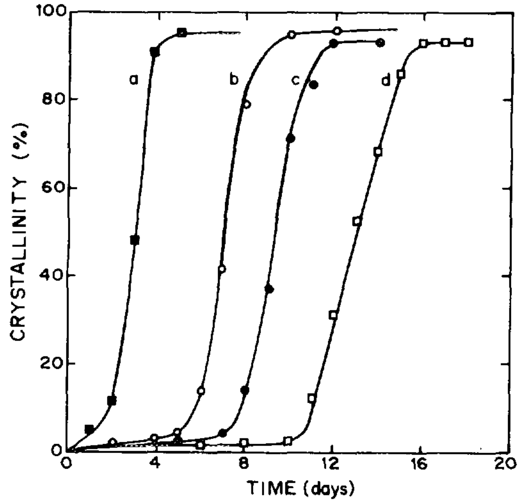


FIG. 1. Hydrothermal crystallization of silica polymorph of NCL-1 (sample A) and vanadium-NCL-1 (samples B, C, and D) ((a) to (d), respectively) with time.

Oxidation of *n*-octane and cyclohexane were carried out in a stirred autoclave (Parr Instrument Company, Illinois, USA) of 300 ml capacity, at 373 K in presence of aqueous $H_2O_2$ (30%) and acetonitrile as solvent. The oxidation of *o*-xylene, *m*-xylene, *p*-xylene, and naphthalene was carried out using the calcined sample C in a batch glass reactor in presence of aqueous $H_2O_2$ and acetonitrile as solvent at 358 K. The reaction products were analyzed by gas chromatography (Hewlett Packard, model 5890 Series II) equipped with a capillary (50 m X 0.25 mm cross linked methyl silicon gum) column. Wherever required some of the products were identified by GC-MS (Shimadzu, model QCMS-QP2000A).

## RESULTS AND DISCUSSION

### *Synthesis*

Figure 1 depicts the course of crystallization of samples A to D (curves (a) to (d), respectively). The percent crystallinity was calculated with reference to the most crystalline sample, from the integrated intensities of all the XRD peaks. The crystallization of Si–NCL-1 (sample A, curve (a)) is complete within 100 h, while vanadium silicates take a longer time. The nucleation and crystallization times increase with the vanadium content (curves b to d for Si/V (input) = 175, 96, and 48, respectively). The powder XRD profiles of the three V–NCL-1 samples (B to D) presented in Fig. 2 match well with that of the V-free silica polymorph (sample A) (curves (b) to (d) and (a), respectively). No peaks other than those already present in the silica polymorph of NCL-1 are observed in the V–NCL-1 samples. Thus, NCL-1, Si–NCL-1, and V–NCL-1 have similar but hitherto unknown crystalline structure. A comparison of the *d* values and intensities of Si–NCL-1 and V–NCL-1 (samples A and D in the calcined and hydrated form) is given Table 1. Preliminary studies indicate orthorhombic symmetry for

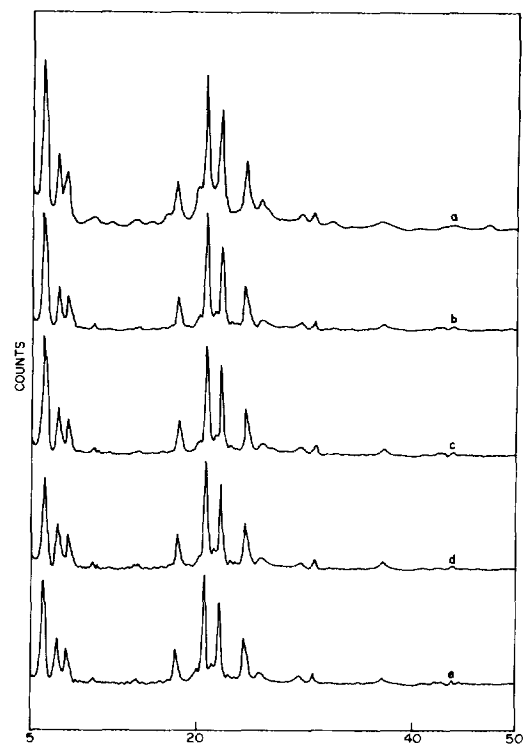


FIG. 2. X-ray diffraction profiles of calcined samples A to D, ((a) to (d), respectively) and of sample after treatment with ammonium acetate and calcination (sample E) (curve (e)).

TABLE 1

XRD Data on Si–NCL-1 and V–NCL-1

| Sample A[a] | | Sample C[b] | | $h$ | $k$ | $l$ |
|---|---|---|---|---|---|---|
| $d$(Å) | $I/I_0$ | $d$(Å) | $I/I_0$ | | | |
| 14.35 | 100 | 14.43 | 100 | 0 | 0 | 2 |
| 11.95 | 25 | 11.98 | 24 | 1 | 0 | 0 |
| 10.92 | 19 | 10.97 | 19 | 1 | 0 | 1 |
| 5.99 | 8 | 6.07 | 10 | 1 | 1 | 0 |
| 4.79 | 32 | 4.79 | 31 | 0 | 0 | 6 |
| 4.18 | 81 | 4.20 | 90 | 0 | 2 | 0 |
| 3.96 | 59 | 3.96 | 69 | 3 | 0 | 0 |
| 3.56 | 38 | 3.58 | 42 | 0 | 0 | 8 |
| 2.87 | 8 | 2.88 | 9 | 0 | 0 | 10 |

[a] Calcined at 823 K.
[b] Calcined at 723 K.

NCL-1 with $a$ = 1.195 ± 0.003, $b$ = 0.836 ± 0.003 and $c$ = 2.870 ± 0.004 nm. The $d$ values calculated on the basis of the above unit cell dimensions compare reasonably well with those observed experimentally (*11*). When the vanadium silicate samples were treated with ammonium acetate and calcined (as described earlier in the Experimental section) there was no significant change in the XRD pattern of the samples (sample E, Fig. 2, curve (e)), indicating the absence of any structural collapse due to treatment with ammonium acetate. The latter is expected to extract out any vanadium present in non-framework positions. Our XRD data show that the crystalline structure is intact even after removal of such vanadium species.

### *Physicochemical Properties*

Table 2 summarizes the physico-chemical properties of all our samples in the calcined form. As-synthesized samples were used for ESR measurements. It is seen that vanadium uptake from the gel during crystallization is far from complete. The efficiency of vanadium incorporation in the final crystalline phase decreases with increasing vanadium content in the starting amorphous gel. When sample D was treated with ammonium acetate and calcined, the resulting material (sample E) had a Si/V ratio of 262, indicating that in sample D part of the vanadium was extractable and, hence, most probably in nonframework positions. Further treatments of sample E with ammonium acetate did not lead to an increase in the Si/V ratio of the sample. The remaining vanadium is apparently firmly bound to the lattice framework and hence cannot be removed by treatment with ammonium acetate. The nitrogen adsorption isotherms at liquid nitrogen temperature indicate that all the samples are typically microporous materials. The mesopore areas (calculated from the $t$-plots) are only about 2.5% of the total apparent surface areas. Micropore structure analysis following the method of Howarth and Kawazoe (*13*) indicate that these samples have an average pore radius of about 0.7 nm. The significant adsorption of $o$-xylene and mesitylene also supports this conclusion (Table 2). The sorption capacity of samples B–D is similar to that of V-free sample A, indicating the absence of any occluded species in the effective void volume of the molecular sieve. The unit cell volume increases linearly with the V/(Si + V) ratio, as can be seen in Fig. 3. When sample D was treated with steam (100%) at 823 K for 4 h, the resulting material (sample F) had the same unit cell volume as the V-free silica polymorph, sample A (2862 vs 2864 Å$^3$, Table 2). The contraction in the unit cell volume on hydrothermal treatment has occurred probably due to the migration of the vanadium ions originally present in framework positions in sample D to nonframework locations.

The probable framework location of most of the vanadium in the NCL-1 structure is suggested from the observation of an IR band at around 960 cm$^{-1}$ for samples B–D. The vanadium-free sample A as well as those wherein vanadium was deposited on sample A do not exhibit this band. Similar observations made in the case of titanium silicalites (TS-1, TS-2, and Ti–ZSM-48) (*14*) and vanadium silicates (V–MFI and

TABLE 2

Physicochemical Properties of V–NCL-1 and Si–NCL-1 Samples

| Samples | Si/V in gel | Si/V in calcined sample | Si/Na | $N_2$ adsorbed[a] vol. (ml/g) (NTP) | Total surface area ($m^2$/g) | Mesopore area ($m^2$/g) | ESR intensity (a.u)[b] | Unit cell volume[c] ($Å^3$) | Sorption capacity[d] (wt%) | |
|---|---|---|---|---|---|---|---|---|---|---|
| | | | | | | | | | o-Xylene | Mesitylene |
| A | — | — | 33 | 77.9 | 339 | 5.4 | — | 2864 | 7.31 | 4.77 |
| B | 175 | 400 | 27 | 70.0 | 298 | 10.0 | 272 | 2883 | 7.28 | 4.68 |
| C | 96 | 250 | 24 | 71.4 | 310 | 8.3 | 371 | 2896 | 7.20 | 4.63 |
| D | 48 | 150 | 20 | 71.4 | 301 | 5.9 | 462 | 2912 | 7.26 | 4.59 |
| E[e] | 48 | 262 | 113 | 73.7 | 311 | 4.3 | 161 | 2891 | — | — |
| F[f] | 48 | — | — | — | — | — | — | 2862 | — | — |

[a] At liquid nitrogen temperature and at $p/p_0$ = 0.1.
[b] Integrated intensity in arbitrary units.
[c] Calculated from the XRD data, of the air calcined samples.
[d] At 298 K and at $p/p_0$ = 0.5; values recorded after 2 h of equilibration.
[e] Sample D treated at 298 K for 24 h with ammonium acetate (50 ml of 0.1 M solution/g catalyst), washed and calcined in air at 723 K, and then reduced in $H_2$ at 703 K.
[f] Sample D treated with steam (100%) at 923 K for 4 h.

V–MEL) (*2, 5*) have been attributed to Si–O–Ti (or V) vibrations, where Ti (or V) is linked to Si–O tetrahedra. The intensity of this absorption is related to the vanadium content in the sample. The ratio of intensity of 960 to 550 $cm^{-1}$ increases linearly with vanadium content as shown in Fig. 4, indicating that most of the vanadium are linked to the silicate lattice structure of NCL-1. The band at 550 $cm^{-1}$ is attributed to structure-sensitive vibrations caused by 5-5 and 5-3 type, double 5-membered ring blocks that are present in pentasil zeolite (ZSM-5 and ZSM-11) structures (*15, 16*). This band develops during the crystallization of zeolites and provides for internal normalization for relative intensity calculations.

The ESR spectra of samples B to D (in the as-synthesized form) (Fig. 5) exhibit anisotropic and eight equally spaced hyperfine splittings indicating the presence of paramagnetic, atomically dispersed, and immobile $V^{4+}$ ions. The integrated ESR intensity

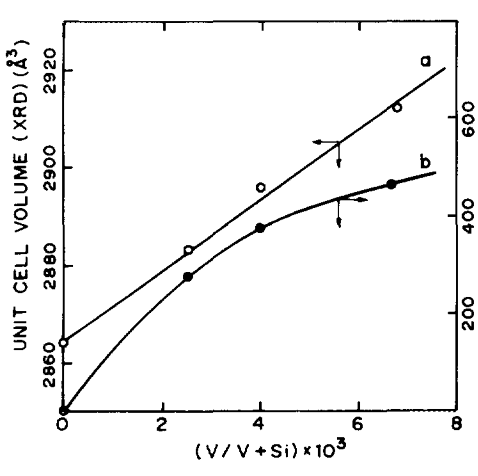


FIG. 3. Correlation between the vanadium content in V–NCL-1 samples and the unit cell volumes (a) and the integrated intensity of ESR signals (b).

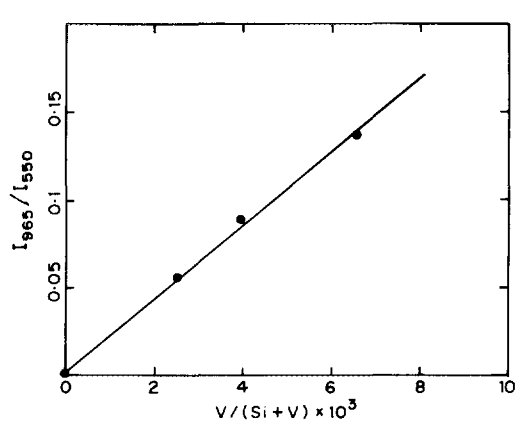


FIG. 4. The ratio of IR intensities at 967 $cm^{-1}$ to that at 550 $cm^{-1}$ vs mole fraction of vanadium in V–NCL-1 samples.

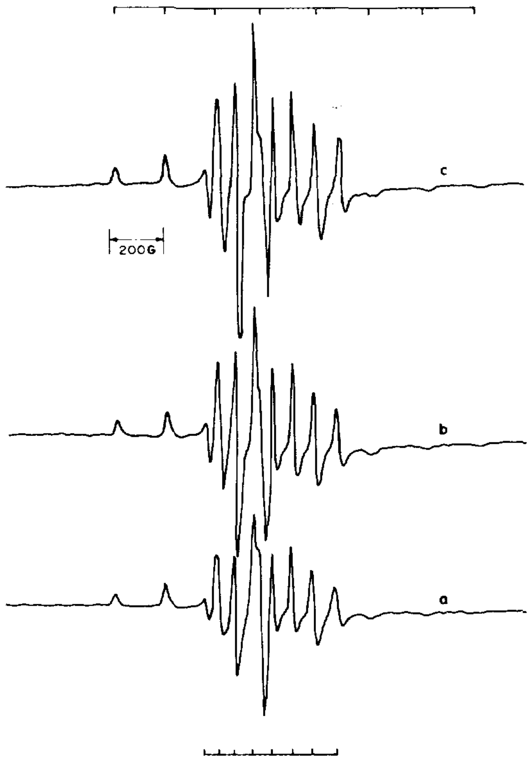


FIG. 5. ESR spectra of as-synthesized V–NCL-1 samples ((a) to (c) refer to samples B to D, respectively).

increased, though not linearly, with the vanadium content in the samples as shown in Fig. 3 (Table 2) The $g$ values and hyperfine coupling constants (A) are given in Table 3, wherein the corresponding values for VS-1 and VS-2 (the vanadium silicate analogs with MFI and MEL structures (7, 9), respectively) are also included. The vanadium silicate samples, after calcination in air, show no ESR signal indicating the oxidation of most of vanadium ions to diamagnetic $V^{5+}$ species (compare curves (a) and (b) in Fig. 6). The flat baseline in curve (a) indicates the absence of $V^{4+}$ clusters in the as-synthesized form. On reduction of the calcined form in $H_2$ at 703 K, the spectrum in curve (c) in Fig. 6 is observed. Reduction converts part of $V^{5+}$ species back to $V^{4+}$ ions. In addition to these isolated $V^{4+}$, the presence of a broad signal (in curve (c)) indicates the formation of cluster-like vanadium species on oxidation–reduction of these vanadium silicates. Apparently, these vanadium clusters are formed on oxidation of the as-synthesized sample. To confirm this hypothesis, the calcined form of sample D (curve (b) in Fig. 6) was treated with ammonium acetate (as described earlier), calcined in air at 723 K and further reduced in $H_2$ at 703 K. The ESR spectrum of the resultant sample is shown in Fig. 6, curve (d). Even though both isolated $V^{4+}$ and vanadium clusters are present, the concentration of the latter is relatively lower (compared to the sample of curve (c)). Treatment with ammonium acetate has removed part of the vanadium clusters formed on calcination of the as-synthesized samples.

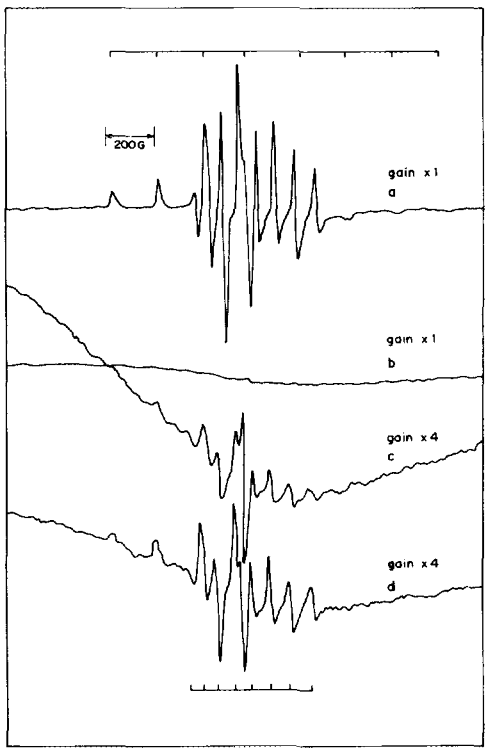


FIG. 6. ESR spectra of as-synthesized V–NCL-1 sample D (a), calcined in air (b), calcined and then reduced in $H_2$ at 703 K for 6 h (c), and calcined in air, treated with ammonium acetate, washed, calcined at 723 K, and then reduced in $H_2$ at 703 K for 6 h (d).

TABLE 3

ESR Parameters of Vanadium-Containing Molecular Sieves[a]

| Samples | Si/V in product | $g_{\parallel}$ | $g_{\perp}$ | $A_{\parallel} \times 10^4$ ($cm^{-1}$) | $A_{\perp} \times 10^4$ ($cm^{-1}$) | References |
|---|---|---|---|---|---|---|
| B (as-synth.) | 400 | 1.935 | 1.972 | 193 | 72.7 | This work |
| C (as-synth.) | 250 | 1.930 | 1.972 | 196 | 71.9 | This work |
| D (as-synth.) | 150 | 1.930 | 1.974 | 196 | 72.1 | This work |
| D1[b] | 150 | 1.934 | 1.980 | 195 | 73.7 | This work |
| *E*[c] | 262 | 1.933 | 1.974 | 194 | 73.6 | This work |
| VS-1 | 42 | 1.949 | 1.990 | 186 | 72.5 | (*7*) |
| VS-2 | 78 | 1.932 | 1.981 | 185 | 72.0 | (*9*) |

[a] Spectra recorded in the X-band at 298 K.

[b] Sample D calcined in air and reduced in $H_2$ at 703 K for 6 h.

[c] Sample D calcined in air and treated with ammonium acetate, washed, calcined at 723 K, and then reduced in $H_2$ at 703 K for 6 h.

In summary, in the as-synthesized form most of the vanadium is present as isolated $V^{4+}$ ions located in framework positions though not necessarily with tetrahedral coordination. On calcination in air the vanadium ions are oxidized to the pentavalent state. In addition, part of the vanadium ions leave lattice locations and form nonframework clusters. Ammonium acetate treatment is able to remove at least part of these clusters. When the oxidized sample is reduced, $V^{4+}$ ions are formed again. While part of these $V^{4+}$ ions are isolated, a significant portion are in cluster-like species. The three-dimensional silicate structure of the molecular sieve is intact during all these treatments. We next discuss the catalytic properties of these materials.

### *Catalytic Activity*

*Oxidation of alkanes.* V–NCL-1 is active in the oxidation of *n*-C6 to *n*-C8 hydrocarbons in the presence of aqueous $H_2O_2$, like VS-2 described earlier (*10*). The results on the oxidation of *n*-octane over sample C are given in Table 4 for illustration. The major products of oxidation are the corresponding alcohols and their secondary oxidation products, viz., the carbonyl compounds (aldehydes and ketones). An interesting observation is the formation of primary alcohols and aldehydes in addition to the secondary alcohols and ketones. Thus, unlike the titanium silicalites, vanadium silicates are able to activate the primary (terminal) carbon atoms of *n*-alkanes (*8*). The product distribu-

TABLE 4

Oxyfunctionalization of *n*-Octane over V–NCL-1[a]

| Catalyst | Sample C |
|---|---|
| Turnover number[b] | 4.6 |
| $H_2O_2$ selectivity[c] (mole %) | 39.5 |
| Product distribution (wt%) | |
| 1-Octanol | 2.1 |
| 2-Octanol | 8.8 |
| 3-Octanol | 4.8 |
| 4-Octanol | 5.2 |
| 1-Octanal | 3.6 |
| 2-Octanone | 22.5 |
| 3-Octanone | 21.1 |
| 4-Octanone | 15.0 |
| Others[d] | 16.9 |

[a] Reaction conditions: catalyst = 0.1 g; *n*-octane = 5 g; alkane/$H_2O_2$ (mole ratio) = 3; solvent (acetonitrile) = 10 g; temperature = 373 K; reaction duration = 8 h.

[b] Moles of reactant converted per mole of vanadium $min^{-1}$.

[c] $H_2O_2$ utilized for monofunctional product formation.

[d] Mostly oxygenates with more than one functional group and lactones.

TABLE 5

Oxidation of Cyclohexane on Vanadium Silicate Molecular Sieves[a]

| Sample | Conv. (mol%) | $H_2O_2$ sel.[b] (mol%) | Product distribution (wt%) | | |
|---|---|---|---|---|---|
| | | | Cyclohexanol | Cyclohexanone | Others[c] |
| D | 11.4 | 48.5 | 33.7 | 60.4 | 5.9 |
| C | 9.7 | 40.1 | 33.4 | 61.3 | 5.3 |
| B | 7.3 | 29.6 | 34.2 | 59.7 | 6.1 |
| A | 2.1 | 3.9 | 16.4 | 18.2 | 65.4 |
| A (impr.)[d] | 2.5 | 4.5 | 15.7 | 17.9 | 66.4 |

[a] Reaction conditions: catalyst = 0.1 g; cyclohexane = 5 g; cyclohexane/$H_2O_2$ (mole ratio) = 3; solvent (acetonitrile) = 20 g; temperature = 373 K; reaction duration = 8 h.
[b] $H_2O_2$ utilized for cyclohexanol and cyclohexanone formation.
[c] Mostly oxygenates with more than one functional group.
[d] 3 wt% of vanadium impregnated on Sample A.

tion shows that the activation of carbon at the second position (among all the secondary carbon atoms) is preferred to others and follows the order 2C > 3C > 4C > 1C.

The influence of Si/V ratio on the oxidation of cyclohexane was studied using calcined samples B, C, and D (Table 5). For comparison, results on V-free Si–NCL-1 (sample A) and sample A impregnated with V are also included in Table 5. As expected, the conversion and $H_2O_2$ selectivity increase with vanadium content, but the product selectivity is similar. However, the increase in the activity is not linearly proportional to the vanadium content of the samples. The three V-catalysts show high selectivity to monofunctional products, viz., cyclohexanol and its secondary oxidation product, cyclohexanone (about 94–95%). The secondary oxidation is faster, the cyclohexanol to cyclohexanone ratio being 0.55 in all the cases. Sample A and V-impregnated sample A, on the other hand, show low activity and yield mainly nonselective oxidation products of cyclohexane. Similar observations have been made on V–MEL samples (*10*).

*Oxidation of alkyl aromatics.* The oxidation of alkyl aromatics leads to ring hydroxylation as well as the oxidation of side chain methyl substituents over samples B–D. The side chain oxidation is preferred to aromatic ring hydroxylation. Thus, in the oxidation of toluene (Table 6), the concentration of (benzyl alcohol + benzaldehyde) is more than that of the cresols (53 vs 46.9 wt%).

TABLE 6

Oxidation of Toluene over V–NCL-1 (Sample C) Molecular Sieve[a]

| Sample | Turnover number[b] | $H_2O_2$ sel.[c] (mol%) | Product distribution (wt%) | | | |
|---|---|---|---|---|---|---|
| | | | Benzyl alcohol | Benzaldehyde | *o*-Cresol | *p*-Cresol |
| C | 0.76 | 39.4 | 7.1 | 46.0 | 31.5 | 15.4 |

[a] Reaction conditions: catalyst = 0.1 g; toluene = 1 g; temperature = 358 K; toluene/$H_2O_2$ (mole ratio) = 3; solvent (acetonitrile) = 10 g; reaction duration = 12 h.
[b] Moles of reactant converted per mole of vanadium $min^{-1}$.
[c] $H_2O_2$ utilized in the formation of benzyl alcohol, benzaldehyde, and cresols.

TABLE 7

Oxidation of Xylene Isomers over V–NCL-1 Molecular Sieve[a]

| Catalyst: | Sample C | | |
|---|---|---|---|
| Substrate: | *o*-Xylene | *m*-Xylene | *p*-Xylene |
| Turnover number[b] | 0.41 | 0.48 | 0.44 |
| $H_2O_2$ selectivity[c] | 34.1 | 32.0 | 36.1 |
| Product distribution, (wt%) | | | |
| 3-Methylbenzyl alcohol | | 42.2 | |
| 3-Methylbenzaldehyde | | 38.9 | |
| 2,6-Dimethylphenol | | 6.9 | |
| 2,4-Dimethylphenol | | 4.5 | |
| 4-Methylbenzyl alcohol | | | 43.0 |
| 4-Methylbenzaldehyde | | | 57.0 |
| 2-Methylbenzyl alcohol | 40.0 | | |
| 2-Methylbenzaldehyde | 60.0 | | |
| Others[d] | | 7.5 | |

[a] Reaction conditions: catalyst = 0.1 g; reactant = 1 g; solvent (acetonitrile) = 10 g; reactant/$H_2O_2$ = 2 moles; temperature = 358 K; reaction duration = 18 h.
[b] Moles of reactants converted per mole of vanadium $min^{-1}$.
[c] $H_2O_2$ utilized for formation of methyl benzyl alcohols, corresponding benzaldehydes, and dimethyl phenols.
[d] Mainly oxygenates with more than one functional group.

Benzaldehyde is formed by the subsequent oxidation of benzyl alcohol. The selectivity to monofunctional products is almost 100%. Being a large pore molecular sieve, there is no steric constraint for the formation of *o*-cresol in V–NCL-1 and the observed *ortho*/*para* ratio of 2.0 is what is expected from purely electronic considerations in the absence of any product shape selectivity. On the other hand, on the medium pore vanadium silicate molecular sieve, VS-2, the formation of *o*-cresol was only marginally higher than that of *p*-cresol, indicating the steric constraints in medium-pore molecular sieves (*8*). The oxidation of benzaldehyde to benzoic acid was not observed in our studies.

In the oxidation of xylenes, conversion and $H_2O_2$ selectivity are similar with the three isomers (Table 7). The products arising out of side chain oxidation predominate. This is in marked contrast to titanium-containing molecular sieves which hydroxylate only the aromatic nucleus giving rise to alkyl phenols (*17*). The pure silica polymorph (sample A) as well as sample A impregnated with vanadium (3 wt%) exhibit only negligible activity. Both *o*- and *p*-xylenes do not undergo ring hydroxylation (no dimethylphenols were detected in the products, Table 7). Apparently, nuclear positions in the aromatic ring are less activated (compared to the side chain alkyl groups) for hydroxylation in these substrates. The oxidation of the methyl substituents in *o*-xylene leads to the formation of 2-methylbenzyl alcohol and 2-methylbenzaldehyde. Similarly, oxidation of *p*-xylene gives almost exclusively 4-methylbenzyl alcohol and the corresponding aldehyde. The selectivity to monofunctional products is almost 100 wt% for both these xylene isomers. On the other hand, oxidation of *m*-xylene leads also to the formation of dimethylphenols (by ring hydroxylation), in addition to giving predominantly 3-methylbenzyl alcohol and the corresponding aldehyde. These results support the view that the hydroxylation of aromatic ring (with $H_2O_2$ as the oxidant) is probably an electrophilic substitution reaction. Bulkier alkyl aromatics like mesitylene are also oxidized over V–NCL-1 (Table 8). Both side-chain oxidation and hydroxylation of the aromatic nucleus occur with mesitylene. Oxidation

TABLE 8

Oxidation of 1,2,4- and 1,3,5-Trimethyl Benzenes over V–NCL-1 (Sample C)[a]

| | Substrate | |
|---|---|---|
| | 1,2,4-Trimethyl benzene | 1,3,5-Trimethyl benzene |
| Turnover number[b] | 0.3 | 0.4 |
| $H_2O_2$ selectivity[c] (mol%) | 28.9 | 33.0 |
| Product distribution (wt%) | | |
| 2,4,6-Trimethyl phenol | | 12.7 |
| 3,5-Dimethyl benzyl alcohol | | 27.2 |
| 3,5-Dimethyl benzaldehyde | | 46.2 |
| 2,4-, 2,5-, 3,4-Dimethyl benzylalcohol | 40.0 | |
| 2,4-, 2,5-, 3,4-Dimethyl benzaldehydes | 51.1 | |
| Others[d] | 8.9 | 13.9 |

[a] Reaction conditions are as given in Table 7.
[b] Moles of reactant converted per mole of vanadium $min^{-1}$.
[c] $H_2O_2$ utilized in the formation of dimethylbenzyl alcohols, corresponding aldehydes and trimethylphenols.
[d] Mainly oxygenates with more than one functional group.

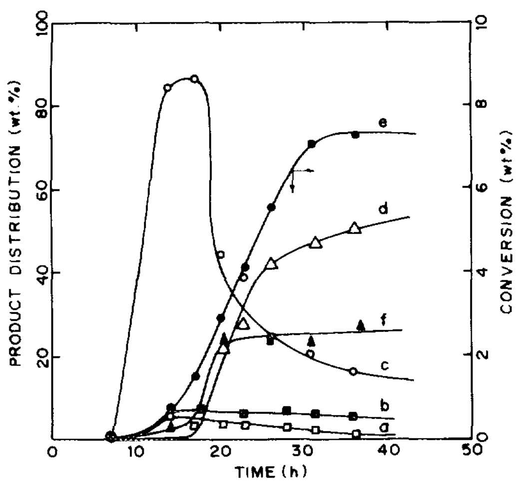


FIG. 7. Oxidation of naphthalene on V–NCL-1 (sample C). The formation of 1-naphthol (a), 2-naphthol (b), 1,4-naphthaquinone (c), phthalic anhydride (d), and others (such as unidentified fragmented products) (f) and conversion (e) in wt% with time.

of 1,2,4-trimethylbenzene leads to products of oxidation of the methyl substituents only.

*Oxidation of naphthalene.* The oxidation of naphthalene over sample C is illustrated in Fig. 7 (Table 9). It may be mentioned here that VS-1 and VS-2 with medium-pore structures do not oxidize such bulky organic substrates including naphthols (*18*). The pure silica polymorph of NCL-1 (sample A) and sample A impregnated with vanadium also do not exhibit this activity. The hydroxylation of naphthalene leads to the formation both 1- and 2-naphthols, as the primary hydroxylation products. Hence, both the 1- and 2-carbon atoms in naphthalene are susceptible to oxidation. The secondary oxidation of 1-naphthol to 1,4-naphthaquinone (via 1,4-dihyroxy naphthalene) appears to be very fast as seen from Fig. 7. A surprising observation is the presence of significant quantities of phthalic anhydride in the product after 23 h. It is formed by the further oxidation of 1,4-naphthaquinones, which is comparatively a slow reaction. The observed maximum in the concentration of 1,4-naphthaquinone and the subsequent increase in that of phthalic anhydride support the sequential nature of these oxidations. This sequence of reactions was confirmed by using 1-naphthol as the substrate. The oxidation of 1-naphthol (7.5 mol% conversion after 18 h reaction) yielded 1,4-naphthaquinone (12.6 wt%) and phthalic anhydride (81.5%).

## CONCLUSIONS

Shape selective oxidation catalysis is a new emerging area. This study has extended

TABLE 9
Oxidation of Naphthalene over V–NCL-1[a]

| Reaction time (h) | Conversion (wt%) | Product distribution (wt%) | | | | |
|---|---|---|---|---|---|---|
| | | 1-Naphthol | 2-Naphthol | 1,4-Naphthoquinone | Phthalic anhydride | Others[b] |
| 7 | 0.0 | — | — | — | — | — |
| 14 | 0.7 | 5.7 | 6.3 | 85.2 | — | 2.9 |
| 17 | 1.5 | 3.1 | 6.8 | 86.9 | — | 2.9 |
| 20 | 2.9 | 3.6 | 5.6 | 44.3 | 22.4 | 24.1 |
| 23 | 3.9 | 3.4 | 5.9 | 39.1 | 27.7 | 23.9 |
| 26 | 5.5 | 2.9 | 6.7 | 24.5 | 42.6 | 23.1 |
| 31 | 7.1 | 2.1 | 6.4 | 20.7 | 47.2 | 23.6 |
| 36 | 7.3 | 0.8 | 5.4 | 16.3 | 50.2 | 27.4 |

[a] Reaction conditions: catalyst = 0.1 g; reactant = 1 g; alkane/$H_2O_2$ (mole ratio) = 2; solvent (acetonitrile) = 10 g; temperature = 358 K.

[b] Mainly fragmented products of naphthalene.

its scope to include the oxidation of bulky molecules, like mesitylene and naphthalene over a novel vanadium silicate molecular sieve with large pores. The location and structure of vanadium in these novel catalysts are far from clear and need further study. Their catalytic properties are quite interesting. They are able to catalyze reactions such as the oxyfunctionalization of the primary carbon atom in alkanes and the side chains in alkyl aromatics. The titanium silicalites (the only other known molecular sieves with shape selective oxidation properties) are not known to catalyze these reactions.

ACKNOWLEDGMENTS

KRR thanks UGC, New Delhi for a fellowship. This study was partly funded by UNDP.

REFERENCES

1. Rigutto, M. S., and Van Bekkum, H., *Appl. Catal.* **68,** L1 (1991).
2. Kornatowski, J., Sychev, M., Goncharuk, V., and Baur, W. H., *Stud. Surf. Sci. Catal.* **65,** 581 (1991).
3. Fejes, P., Marsi, I., Kiricsi, I., Halasz, J., Hannus, I., Rockenbauer, A., Tasi, Gy., Korecz L., and Schobel, Gy., *Stud. Surf. Sci. Catal.* **69,** 173 (1991).
4. Centi, G., Perathoner, S., Trifiro, F., Aboukais, A., Aissi C. F., and Guelton, M., *J. Phys. Chem.* **96,** 2617 (1992).
5. Hari Prasad Rao, P. R., Ramaswamy, A. V., and Ratnasamy, P., *J. Catal.* **137,** 225 (1992).
6. Montes, C., Davis, M. E., Murry B., and Narayana, M., *J. Phys. Chem.* **94,** 6431 (1990).
7. Hari Prasad Rao, P. R., and Ramaswamy, A. V., *Appl. Catal. A: General* **93,** 123 (1993).
8. Hari Prasad Rao, P. R., and Ramaswamy, A. V., *J. Chem. Soc. Chem. Commun.*, 1245 (1992).
9. Hari Prasad Rao, P. R., Belhekar, A. A., Hegde, S. G., Ramaswamy, A. V., and Ratnasamy, P., *J. Catal.* **141,** 595 (1993).
10. Hari Prasad Rao, P. R., Ramaswamy, A. V., and Ratnasamy, P., *J. Catal.* **141,** 604 (1993).
11. Kumar, R., Reddy, K. R., Raj A., and Ratnasamy, P., 9th International Zeolite Conference, Montreal, Canada, Paper A6 (1992); Kumar, R., Reddy, K. R., and Ratnasamy, P., Indian Patent Appl. No. 766/DEL/91; Kumar, R., Reddy K. R., and Ratnasamy, P., EP Appl. No. 92300166.3.
12. Ramesh Reddy, K., Ramaswamy, A. V., and Ratnasamy, P., *J. Chem. Soc. Chem. Commun.*, 1613 (1992).
13. Howarth, G., and Kawazoe, K., *J. Chem. Soc. Jpn.* **16,** 470 (1983).
14. Serrano, D. P., Hong-Xin Li, and Davis, M. E., *J. Chem. Soc. Chem. Commun.*, 745 (1992).
15. Jacobs, P. A., Beyer, H. K., and Valyan, J., *Zeolites* **1,** 161 (1981).
16. Coudurier, G., Naccache, C., and Vedrine, J. C., *J. Chem. Soc. Chem. Commun.*, 1413 (1982).
17. Reddy, J. S., and Sivasanker, S., *Indian J. Technol.* **30,** 64 (1992).
18. Hari Prasad Rao, P. R., and Ramaswamy, A. V., unpublished results.